Tuberculosis Detection in X-Ray Image Using Deep Learning Approach with VGG-16 Architecture

Suci Aulia, Sugondo Hadiyoso
School of Applied Science, Telkom University, Bandung 40257, Indonesia

ARTICLE INFO

Article history:

Received May 25, 2022
Revised June 24, 2021
Accepted July 26, 2021

Keywords:

Tuberculosis;
X-ray;
Detection;
CNN;
VGG

ABSTRACT

Tuberculosis (TB) is a chronic disease still the main problem in Indonesia. However, this disease can be cured with drugs at a particular time after the patient is detected as having TB. TB diagnosis or screening can be made through x-ray imaging of the chest cavity by a radiology specialist. The Mantoux test can then be used to confirm the diagnosis. X-ray images often have varying contrasts that lead to true negatives or false negatives. Whereas generally, a chest x-ray is the initial examination of TB. Error detection will have a fatal impact on treatment therapy. Therefore, this study proposed a system for TB detection based on x-ray images using deep learning. The system developed uses a Convolutional Neural Network (CNN) with the VGG-16 architecture. In the performance test stage, 700 normal and 140 TB chest x-ray images were used. The simulation results show that the proposed system can classify normal and TB lungs with an accuracy of 99.76%. The highest accuracy is achieved using batch size=50. This system is expected to assist radiology in detecting tuberculosis on X-Ray images of the lungs. The contribution of this study is to build a machine learning model for TB detection and optimization of model parameters to get the best accuracy.

Corresponding Author:

Sugondo Hadiyoso, Telkom University, Telekomunikasi No. 1, Bandung 40257, Indonesia
Email: sugondo@telkomuniversity.ac.id

1. INTRODUCTION

Tuberculosis (TB) is one of the endemic diseases in Indonesia, with the third-highest number of sufferers after India and China [1]. It is an acute and chronic disease over time [2]. TB can affect everyone, both adults and children. It can affect physical growth in children because TB bacteria absorb nutrients from food. The Indonesian government has consistently fought TB to reduce the number of sufferers and mortality rates by providing free treatment. Early detection of TB is an essential protocol for determining cure therapy [3]. TB is diagnosed by medical imaging of the chest cavity or the use of reagents that react with TB bacteria [4].

Over the past decade, x-ray imaging has been used to screen for TB. Early evaluation of an ultra-portable x-ray system for active tuberculosis case finding [5]. Some underlying factors are high sensitivity, cheapness, and non-invasive. Radiology specialists have been manually observing chest x-ray images to determine the presence or absence of bacterial bundles in the lungs. However, this tends to be subjective and depends on the clinician's experience. The quality of the x-ray image also greatly determines the accuracy of the diagnosis because the gray x-ray image tends to be faint.

Digital image processing techniques have an essential role in the medical field, such as image reconstruction [6][7], compression [8][9], image enhancement [10], and classification or detection [11]. Computer application for disease detection or classification is one of the areas that has received the most attention. Numerous studies have proposed methods for classifying medical images to help diagnose a disease.

Recently, studies on the detection of TB based on chest x-ray have been reported. The study of TB detection from chest x-rays using five artificial intelligence algorithms by Qin et al. showed a sensitivity of about 90% [12]. In another study by Liebenlito et al., performing chest x-rays classification of TB and pneumonia using the convolutional neural network (CNN) resulted in 86% accuracy in identifying TB [13]. A similar study on chest x-ray classification of TB cases using CNN generating an accuracy of >80 to 92.5% has been reported [14][15]. Some of the literature shows that TB detection studies are still an important issue, especially with the CNN approach [16][17]. However, there is still a gap in improving accuracy. The datasets used are also diverse so that previous studies can mutually reinforce one another. In addition, testing with large amounts of data is also required.

In this study, a method for detecting tuberculosis based on chest x-ray images is proposed using a convolutional neural network. The CNN architecture employed in this simulation is VGG by changing several parameters to get the best performance. X-ray images consist of normal and tuberculosis sourced from open datasets. The parameters of the proposed test method include accuracy, precision, recall, and F1 score. The contribution of this study is to build a machine learning model for TB detection on chest x-ray and optimization of model parameters to get the highest accuracy. With this proposed method, it is hoped that it can support the achievements of previous studies so that they can strengthen the diagnosis of TB using digital analysis.

2. MATERIAL AND METHODS

2.1. System Overview

Fig. 1 shows the proposed system for TB detection based on the chest x-ray image [18]. First, the original chest x-ray image from the database is resized to 64×64 pixels. Furthermore, feature extraction is carried out using CNN with the VGG-16 architecture. The model learning process is also carried out at this stage. The last is whether TB or normal based on training on the built model. Several parameter modification scenarios are carried out to determine the system's best performance. The simulation in this study uses pythons that are run on Google Colab. An explanation of the input image, CNN method, and performance evaluation are presented in the following sub-section.

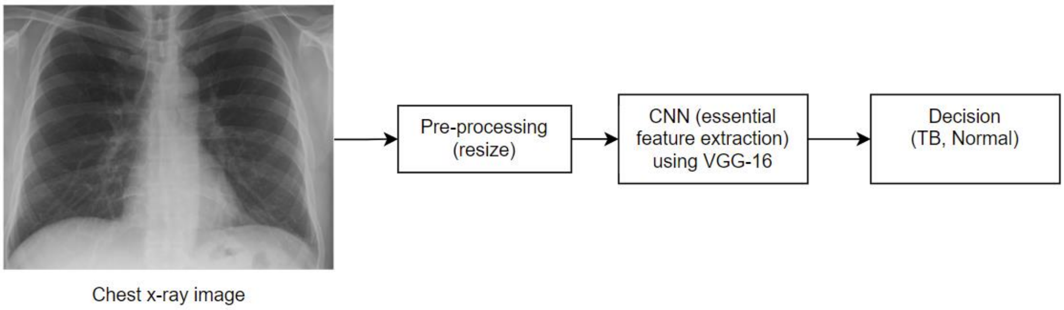

Fig. 1. The proposed system for TB and normal classification chest x-ray image

2.2. Normal and TB Chest X-Ray Dataset

Chest x-ray, both normal and TB, are sourced from an open dataset which can be downloaded at https://www.kaggle.com/datasets/tawsifurrahman/tuberculosis-tb-chest-xray-dataset [19]. A research team collected this database from Qatar University, Qatar, University of Dhaka, Bangladesh, researchers from Malaysia, and in collaboration with doctors from Hamad Medical Corporation and Bangladesh. This database consists of 700 TB chest x-rays and 3500 normal chest x-rays. An example of TB and a normal chest x-ray is presented in Fig. 2. The expert radiologist annotated both normal and abnormal.

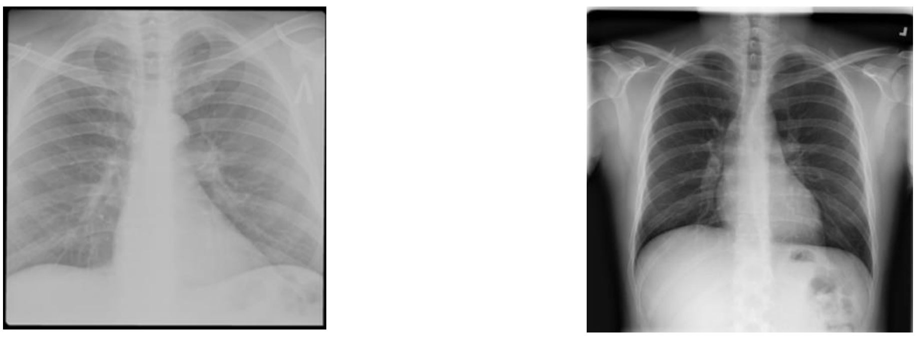

(a) (b)

Fig. 2. Chest x-ray (a) TB (b) normal

The TB image consisted of 306 images from the BELARUS dataset and 394 images from the NLM dataset. Meanwhile, normal images consist of 406 images from NLM, and 3094 images are from RSNA. Then normal and TB were collected into an open dataset [20]. Chest x-ray images with a resolution of 512×512 pixels are then saved. PNG format.

2.3. Convolutional Neural Network

A convolutional Neural Network (CNN) is one of the most common types of deep learning (DL) algorithms used for processing image or array data [21]. The term CNN refers to the convolution operation in the recognition process with multi-layer convolution [22]. The output is in the form of features extracted from the input image. CNN's architecture is similar to the pattern of connections in the human brain's neurons, inspired by the visual cortex, which functions to process visuals [23]. The general form of the CNN architecture is presented in Fig. 3.

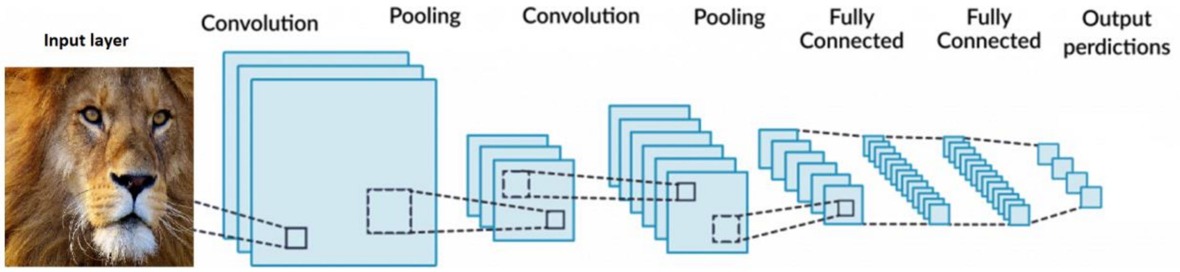

Fig. 3. The basic concept of CNN architecture

CNN consists of convolutional layers, pooling layers, and fully connected (FC) layers [24][25]. They have functions for feature extraction represented by convolutional layers and pooling layers, while fully connected (FC) layers perform classification functions [26][27]. In its application, CNN has been developed into various architectures such as ResNet, VGG, DenseNet, AlexNet, ChexNet, Inception, MobileNet, and others. In this study, the CNN architecture employed is VGG-16.

2.4. Visual Geometry Group (VGG)-16 Architecture

The VGG-16 architecture is one of the popular CNN architectures and is widely used in image recognition development [28][29]. This architecture is an improvement of AlexNet [30][31]. The basic concept of VGG-16 is using a convolutional filter with a size of 3×3 [32]. Thus, it can produce essential features so that it becomes more accurate [33]. The VGG-16 architecture has 16 layers consisting of 13 convolutional layers and three fully connected layers. The VGG-16 architecture is illustrated in Fig. 4.

An overview of each component of the VGG-16 architecture is as follows:

- Input layer: the input image is resized to 64×44.
- Convolutional Layers: The convolutional filter kernel is 3×3 in size [34]. Apart from that, there is also a 1×1 convolution filter that acts as a linear input transformation. This section also includes a ReLU unit to speed up compute time compared to processing on AlexNet.
- Fully Connected Layers: The VGG-16 has three fully connected layers [35]. The first two have 4096 channels of the three layers, and the third has 1000 channels.

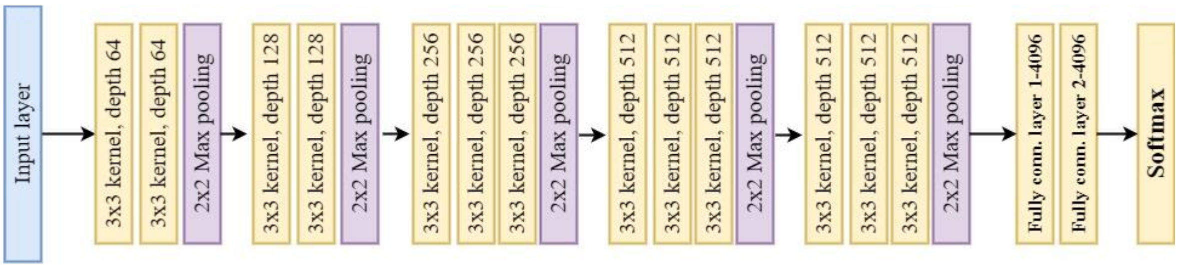

Fig. 4. VGG-16 Architecture

2.5. Performance Evaluation

In this study, the evaluation of the performance system in TB detection is included: accuracy, precision, recall, and F1-score. These performance parameters are calculated using the following equation (1-4) [36][37]:

$$Accuracy = \frac{TP + TN}{TP + TN + FP + FN} \tag{1}$$

$$Precision = \frac{TP}{TP + FP} \tag{2}$$

$$Recall = \frac{TP}{TP + FN} \tag{3}$$

$$F1 - score = \frac{2 * Precision * Recall}{Precision + Recall} \tag{4}$$

Where, True positive (TP) is defined as positive data that is predicted to be correct, and true negative (TN) is defined as negative data that is predicted to be correct. Meanwhile, false positive (FP) is negative data but predicted as positive data, and false negative (FN) is positive data but predicted as negative data [38][39].

3. RESULTS AND DISCUSSION

Each image was rescaled to 64×64×3 (weigh × heigh × 3 layers RGB). VGG-16 was implemented in training and testing to classify the Chest x-ray images into normal and tuberculosis. The VGG-16 model used in this study has a model design, as seen in Fig. 5, as details of the summary of the model are in Fig. 6.

```
model = vgg16.output
model = tf.keras.layers.GlobalMaxPooling2D()(model)
model = tf.keras.layers.Flatten()(model)
model = tf.keras.layers.Dense(512,activation='relu')(model)
model = tf.keras.layers.Dropout(rate=0.25)(model)
model = tf.keras.layers.Dense(2,activation='softmax')(model)
model = tf.keras.models.Model(inputs=vgg.input, outputs = model)
```

Fig. 5. VGG-16 model design

The simulation results with several epoch and batch size scenarios are presented in Table 1. Based on the test results data carried out, the highest accuracy of the VGG-16 method in classifying pulmonary tuberculosis can reach 99.76% with 100% precision and an F1 score. The best performance was obtained using epoch=1 and batch size=50. Batch size is a reflection of the number of training iterations. The simulation results show that the larger batch size can produce higher accuracy, and the most optimal use of batch size is 50. With a batch size is 60, the performance decreases because there is a possibility of bias in the learning process. The confusion matrix measurement details from the highest accuracy are shown in Fig. 7. The validation stage used 700 normal and 140 TB chest x-rays. The classification simulation showed that all normal chest x-rays were detected 100%. Meanwhile, it was found that two TB x-ray images were predicted to be normal. The resulting detection error is not more than 1%.

Table 1. Experimental results based on the effect of epoch and batch size parameters

Epoch	Batch_size	Accuracy (%)	Loss (%)	Precision (%)	Recall (%)	F1-Score (%)
2	20	98.57	6.07	99	96	97
1	40	97.62	5.20	99	96	97
2	40	99.52	1.21	99	99	99
3	40	98.57	3.27	96	99	97
1	50	99.76	1.78	100	99	100
2	50	99.29	2.43	99	99	99
3	50	99.64	1.28	99	99	99
5	60	99.29	2.89	100	98	99

```
Layer (type)                 Output Shape              Param #
=================================================================
input_1 (InputLayer)         [(None, 64, 64, 3)]       0

block1_conv1 (Conv2D)        (None, 64, 64, 64)        1792

block1_conv2 (Conv2D)        (None, 64, 64, 64)        36928

block1_pool (MaxPooling2D)   (None, 32, 32, 64)        0

block2_conv1 (Conv2D)        (None, 32, 32, 128)       73856

block2_conv2 (Conv2D)        (None, 32, 32, 128)       147584

block2_pool (MaxPooling2D)   (None, 16, 16, 128)       0

block3_conv1 (Conv2D)        (None, 16, 16, 256)       295168

block3_conv2 (Conv2D)        (None, 16, 16, 256)       590080

block3_conv3 (Conv2D)        (None, 16, 16, 256)       590080

block3_pool (MaxPooling2D)   (None, 8, 8, 256)         0

block4_conv1 (Conv2D)        (None, 8, 8, 512)         1180160

block4_conv2 (Conv2D)        (None, 8, 8, 512)         2359808

block4_conv3 (Conv2D)        (None, 8, 8, 512)         2359808

block4_pool (MaxPooling2D)   (None, 4, 4, 512)         0

block5_conv1 (Conv2D)        (None, 4, 4, 512)         2359808

block5_conv2 (Conv2D)        (None, 4, 4, 512)         2359808

block5_conv3 (Conv2D)        (None, 4, 4, 512)         2359808

block5_pool (MaxPooling2D)   (None, 2, 2, 512)         0

global_max_pooling2d (Globa   (None, 512)              0
lMaxPooling2D)

flatten (Flatten)            (None, 512)               0

dense (Dense)                (None, 512)               262656

dropout (Dropout)            (None, 512)               0

dense_1 (Dense)              (None, 2)                 1026

=================================================================
Total params: 14,978,370
Trainable params: 14,978,370
Non-trainable params: 0
```

Fig. 6. The VGG-16 model summary from the training process

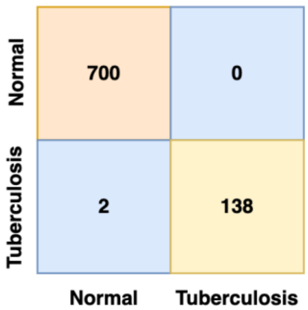

Fig. 7. The confusion matrix on epoch = 1, and batch size = 50

The proposed method has a better performance than previous studies for the classification of tuberculosis based on x-ray images. As presented in Table 2, our proposed method is approved that has the highest accuracy, precision, recall, and F1 score among two other studies. Results performance measurement based on our proposed method is also visually proven to be better than others, as shown in Fig. 8.

Table 2. Comparison of classification results with previous studies

No	Studies	Accuracy (%)	Precision (%)	Recall (%)	F1-Score (%)
1.	**Proposed**	**99.76**	**100**	**99**	**100**
2.	[15]	89	85	91	89
3.	[40]	90	90	90	90
4.	[41]	90	-	-	-

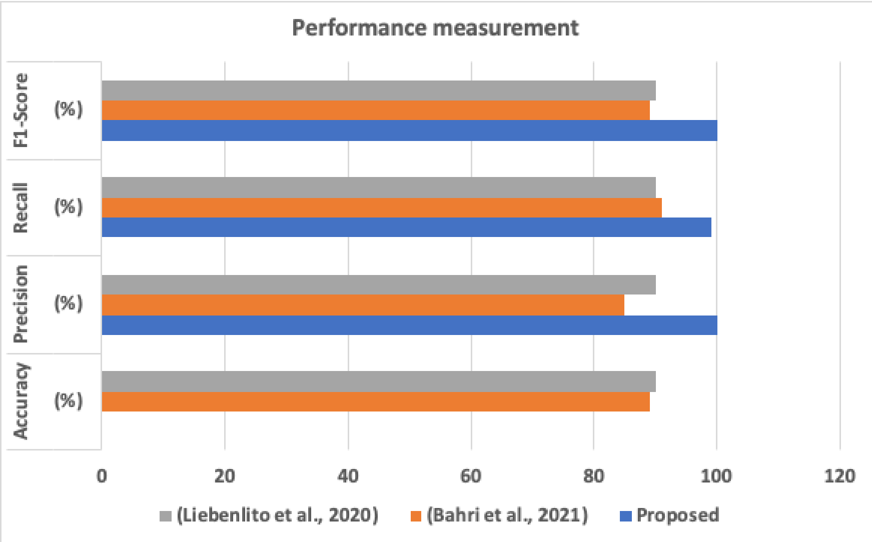

Fig. 8. The comparison of results performance measurement

4. CONCLUSION

In this study, a method for detecting tuberculosis based on chest x-ray images is proposed using a convolutional neural network. The CNN architecture employed in this simulation is VGG by changing several parameters to get the best performance. X-ray images consist of normal and tuberculosis sourced from open datasets. The parameters of the proposed test method include accuracy, precision, recall, and F1 score. The system developed uses a convolutional neural network (CNN) based on the VGG-16 architecture. The simulation results show that the proposed system can classify normal and TB lungs with accuracy, precision, recall, and F1 score are 99.76%, 100%, 99%, and 100%, respectively. This system is expected to assist radiology in detecting tuberculosis on X-Ray images of the lungs. This proposed method achieves the highest performance among the previous studies so that they can strengthen the diagnosis of TB using digital analysis. Based on WHO standards, TB positive consists of several categories such as scanty, TB +1, TB +2, and TB+3, according to the International Union against Tuberculosis and Lung Disease (IUATLD) levels. Therefore, this classification according to WHO standards are a challenge in our future work to classify TB x-ray images into IUATLD levels.

REFERENCES

[1] T. N. Susilawati and R. Larasati, "A recent update of the diagnostic methods for tuberculosis and their applicability in Indonesia: a narrative review," *Med J Indones*, vol. 28, no. 3, pp. 284–91, Oct. 2019, https://doi.org/10.13181/mji.v28i3.2589.

[2] J. L. de O. Magalhães, J. F. da C. Lima, A. A. de Araújo, I. O. Coutinho, N. C. Leal, and A. M. P. de Almeida, "Microscopic detection of Mycobacterium tuberculosis in direct or processed sputum smears," *Rev. Soc. Bras. Med. Trop.*, vol. 51, no. 2, pp. 237–239, Apr. 2018, https://doi.org/10.1590/0037-8682-0238-2017.

[3] I. W. G. A. E. Putra *et al.*, "The Implementation of Early Detection in Tuberculosis Contact Investigation to Improve Case Finding," *JEGH*, 2019, https://doi.org/10.2991/jegh.k.190808.001.

[4] S. Aulia, S. Hadiyoso, T. L. E. R. Mengko, and A. B. Suksmono, "Covid-19 and Tuberculosis Classification Based on Chest X-Ray Using Convolutional Neural Network," in *Proceedings of the 1st International Conference on Electronics, Biomedical Engineering, and Health Informatics*, vol. 746, 2021, pp. 407–420, https://doi.org/10.1007/978-981-33-6926-9_35.

[5] L. N. Q. Vo *et al.*, "Early Evaluation of an Ultra-Portable X-ray System for Tuberculosis Active Case Finding," *TropicalMed*, vol. 6, no. 3, p. 163, Sep. 2021, https://doi.org/10.3390/tropicalmed6030163.

[6] I. Dyah Irawati, S. Hadiyoso, and A. Fahmi, "Compressive Sensing in Lung Cancer Images for Telemedicine Application," in *The 4th International Conference on Electronics, Communications and Control Engineering*, Seoul Republic of Korea, Apr. 2021, pp. 55–61, https://doi.org/10.1145/3462676.3462685.
[7] Y. S. Perkasa, K. N. Syaja'ah, L. Ismadelani, and R. D. Agustina, "Reconstruction of High Resolution Medical Image Using General Regression Neural Network (GRNN)," *J. Penelit. Fis. Apl.*, vol. 10, no. 2, p. 137, Dec. 2020, https://doi.org/10.26740/jpfa.v10n2.p137-145.
[8] G. Xin and P. Fan, "A lossless compression method for multi-component medical images based on big data mining," *Sci Rep*, vol. 11, no. 1, p. 12372, Dec. 2021, https://doi.org/10.1038/s41598-021-91920-x.
[9] D. Yee, S. Soltaninejad, D. Hazarika, G. Mbuyi, R. Barnwal, and A. Basu, "Medical image compression based on region of interest using better portable graphics (BPG)," in *2017 IEEE International Conference on Systems, Man, and Cybernetics (SMC)*, Banff, AB, Oct. 2017, pp. 216–221, https://doi.org/10.1109/SMC.2017.8122605.
[10] D. Eun, R. Jang, W. S. Ha, H. Lee, S. C. Jung, and N. Kim, "Deep-learning-based image quality enhancement of compressed sensing magnetic resonance imaging of vessel wall: comparison of self-supervised and unsupervised approaches," *Sci Rep*, vol. 10, no. 1, p. 13950, Dec. 2020, https://doi.org/10.1038/s41598-020-69932-w.
[11] S. U. K. Bukhari, A. Syed, S. K. A. Bokhari, S. S. Hussain, S. U. Armaghan, and S. S. H. Shah, "The Histological Diagnosis of Colonic Adenocarcinoma by Applying Partial Self Supervised Learning," *Pathology*, Aug. 2020, https://doi.org/10.1101/2020.08.15.20175760.
[12] Z. Z. Qin *et al.*, "Tuberculosis detection from chest x-rays for triaging in a high tuberculosis-burden setting: an evaluation of five artificial intelligence algorithms," *The Lancet Digital Health*, vol. 3, no. 9, pp. e543–e554, Sep. 2021, https://doi.org/10.1016/S2589-7500(21)00116-3.
[13] M. Liebenlito, Y. Irene, and A. Hamid, "Classification of Tuberculosis and Pneumonia in Human Lung Based on Chest X-Ray Image using Convolutional Neural Network," *InPrime: Ind. Jour. Pure. Applied. Math*, vol. 2, no. 1, pp. 24–32, Mar. 2020, https://doi.org/10.15408/inprime.v2i1.14545.
[14] M. Ahsan, R. Gomes, and A. Denton, "Application of a convolutional neural network using transfer learning for tuberculosis detection," *IEEE International Conference on Electro Information Technology*, vol. 2019-May, pp. 427–433, 2019, https://doi.org/10.1109/EIT.2019.8833768.
[15] S. Bahri, R. Wajhillah, and M. F. Adiwisastra, "Diagnosa Tuberculosis Paru Berbasis Citra X-ray," *Indonesian Journal on Computer and Information Technology*, vol. 6, no. September, pp. 181–186, 2021.
[16] F. Pasa, V. Golkov, F. Pfeiffer, D. Cremers, and D. Pfeiffer, "Efficient Deep Network Architectures for Fast Chest X-Ray Tuberculosis Screening and Visualization," *Sci Rep*, vol. 9, no. 1, p. 6268, Dec. 2019, https://doi.org/10.1038/s41598-019-42557-4.
[17] A. U. Ibrahim, E. Guler, M. Guvenir, K. Suer, S. Serte, and M. Ozsoz, "Automated detection of Mycobacterium tuberculosis using transfer learning," J. Infect. Dev. Ctries., vol. 15, no. 5, pp. 678–686, 2021, https://doi.org/10.3855/jidc.13532.
[18] G. Tavaziva *et al.*, "Diagnostic accuracy of a commercially-available, deep learning-based chest-Xray interpretation software for detecting culture-confirmed pulmonary tuberculosis," *International Journal of Infectious Diseases*, p. S1201971222002983, May 2022, https://doi.org/10.1016/j.ijid.2022.05.037.
[19] T. Rahman *et al.*, "Reliable Tuberculosis Detection Using Chest X-Ray With Deep Learning, Segmentation and Visualization," *IEEE Access*, vol. 8, pp. 191586–191601, 2020, https://doi.org/10.1109/ACCESS.2020.3031384.
[20] T. Rahman *et al.*, "Reliable tuberculosis detection using chest X-ray with deep learning, segmentation and visualization," *IEEE Access*, vol. 8, no. October, pp. 191586–191601, 2020, https://doi.org/10.1109/ACCESS.2020.3031384.
[21] T. M. Saravanan, K. Karthiha, R. Kavinkumar, S. Gokul, and J. P. Mishra, "A novel machine learning scheme for face mask detection using pretrained convolutional neural network," *Materials Today: Proceedings*, vol. 58, pp. 150–156, 2022, https://doi.org/10.1016/j.matpr.2022.01.165.
[22] S. Ji, W. Li, B. Zhang, L. Zhou, and C. Duan, "Bucket Teeth Detection Based on Faster Region Convolutional Neural Network," *IEEE Access*, vol. 9, pp. 17649–17661, 2021, https://doi.org/10.1109/ACCESS.2021.3054436.
[23] T. M. Saravanan, K. Karthiha, R. Kavinkumar, S. Gokul, and J. P. Mishra, "A novel machine learning scheme for face mask detection using pretrained convolutional neural network," *Materials Today: Proceedings*, vol. 58, pp. 150–156, 2022, https://doi.org/10.1016/j.matpr.2022.01.165.
[24] F.-C. Chen and M. R. Jahanshahi, "NB-CNN: Deep Learning-Based Crack Detection Using Convolutional Neural Network and Naïve Bayes Data Fusion," *IEEE Trans. Ind. Electron.*, vol. 65, no. 5, pp. 4392–4400, May 2018, https://doi.org/10.1109/TIE.2017.2764844.
[25] Y. Jing, L. Zhang, W. Hao, and L. Huang, "Numerical study of a CNN-based model for regional wave prediction," *Ocean Engineering*, vol. 255, p. 111400, Jul. 2022, https://doi.org/10.1016/j.oceaneng.2022.111400.
[26] C. Adak, S. Marinai, B. B. Chaudhuri, and M. Blumenstein, "Offline Bengali Writer Verification by PDF-CNN and Siamese Net," in *2018 13th IAPR International Workshop on Document Analysis Systems (DAS)*, Apr. 2018, pp. 381–386, https://doi.org/10.1109/DAS.2018.33.
[27] R. Hou, C. Chen, and M. Shah, "Tube Convolutional Neural Network (T-CNN) for Action Detection in Videos," in *2017 IEEE International Conference on Computer Vision (ICCV)*, Venice, Oct. 2017, pp. 5823–5832, https://doi.org/10.1109/ICCV.2017.620.
[28] Z. Song, L. Fu, J. Wu, Z. Liu, R. Li, and Y. Cui, "Kiwifruit detection in field images using Faster R-CNN with VGG16," *IFAC-PapersOnLine*, vol. 52, no. 30, pp. 76–81, 2019, https://doi.org/10.1016/j.ifacol.2019.12.500.

[29] N. K. Mishra, P. Singh, and S. D. Joshi, "Automated detection of COVID-19 from CT scan using convolutional neural network," *Biocybernetics and Biomedical Engineering*, vol. 41, no. 2, pp. 572–588, Apr. 2021, https://doi.org/10.1016/j.bbe.2021.04.006.
[30] S. S. Verma, A. Prasad, and A. Kumar, "CovXmlc: High performance COVID-19 detection on X-ray images using Multi-Model classification," *Biomedical Signal Processing and Control*, vol. 71, p. 103272, Jan. 2022, https://doi.org/10.1016/j.bspc.2021.103272.
[31] L. Kong and J. Cheng, "Classification and detection of COVID-19 X-Ray images based on DenseNet and VGG16 feature fusion," *Biomedical Signal Processing and Control*, vol. 77, p. 103772, Aug. 2022, https://doi.org/10.1016/j.bspc.2022.103772.
[32] N. Deepa and S. P. Chokkalingam, "Optimization of VGG16 utilizing the Arithmetic Optimization Algorithm for early detection of Alzheimer's disease," *Biomedical Signal Processing and Control*, vol. 74, p. 103455, Apr. 2022, https://doi.org/10.1016/j.bspc.2021.103455.
[33] A. A. Pravitasari, N. Iriawan, U. S. Nuraini, and D. A. Rasyid, "On comparing optimizer of UNet-VGG16 architecture for brain tumor image segmentation," in *Brain Tumor MRI Image Segmentation Using Deep Learning Techniques*, Elsevier, 2022, pp. 197–215, https://doi.org/10.1016/B978-0-323-91171-9.00004-1.
[34] D. Jayadevappa, S. Ingaleshwar, and S. Kumar, "Comparative analysis of deformable models based segmentation methods for brain tumor classification," in *Brain Tumor MRI Image Segmentation Using Deep Learning Techniques*, Elsevier, 2022, pp. 215–225, https://doi.org/10.1016/B978-0-323-91171-9.00011-9.
[35] S. Dey, R. Roychoudhury, S. Malakar, and R. Sarkar, "An optimized fuzzy ensemble of convolutional neural networks for detecting tuberculosis from Chest X-ray images," *Applied Soft Computing*, vol. 114, p. 108094, Jan. 2022, https://doi.org/10.1016/j.asoc.2021.108094.
[36] A. S. Musallam, A. S. Sherif, and M. K. Hussein, "Efficient framework for detecting COVID-19 and pneumonia from chest X-ray using deep convolutional network," *Egyptian Informatics Journal*, p. S1110866522000020, Feb. 2022, https://doi.org/10.1016/j.eij.2022.01.002.
[37] D. K. Atal and M. Singh, "Arrhythmia Classification with ECG signals based on the Optimization-Enabled Deep Convolutional Neural Network," *Computer Methods and Programs in Biomedicine*, vol. 196, p. 105607, Nov. 2020, https://doi.org/10.1016/j.cmpb.2020.105607.
[38] A. Elazab, M. A. Elfattah, and Y. Zhang, "Novel multi-site graph convolutional network with supervision mechanism for COVID-19 diagnosis from X-ray radiographs," *Applied Soft Computing*, vol. 114, p. 108041, Jan. 2022, https://doi.org/10.1016/j.asoc.2021.108041.
[39] S. Showkat and S. Qureshi, "Efficacy of Transfer Learning-based ResNet models in Chest X-ray image classification for detecting COVID-19 Pneumonia," *Chemometrics and Intelligent Laboratory Systems*, vol. 224, p. 104534, May 2022, https://doi.org/10.1016/j.chemolab.2022.104534.
[40] M. Liebenlito, Y. Irene, and A. Hamid, "Classification of Tuberculosis and Pneumonia in Human Lung Based on Chest X-Ray Image using Convolutional Neural Network," *InPrime: Indonesian Journal of Pure and Applied Mathematics*, vol. 2, no. 1, pp. 24–32, 2020, https://doi.org/10.15408/inprime.v2i1.14545.
[41] Z. Z. Qin *et al.*, "Tuberculosis detection from chest x-rays for triaging in a high tuberculosis-burden setting: an evaluation of five artificial intelligence algorithms," *The Lancet. Digital health*, vol. 3, no. 9, pp. e543–e554, 2021, https://doi.org/10.1016/S2589-7500(21)00116-3.

BIOGRAPHY OF AUTHORS

Suci Aulia received the Master in Electrical-Telecommunication Engineering from Telkom University, Bandung, Indonesia, in June 2012. Her research interests are image processing, biomedical imaging, and computer vision. At 2020-present, she became a doctoral student in electrical engineering at the Bandung Institute of Technology. Her doctoral research focuses on biomedical imaging and analysis of pulmonary tuberculosis diagnosis. Email: suciaulia@telkomuniversity.ac.id, Orchid: https://orcid.org/0000-0003-0568-4424.

Sugondo Hadiyoso received a Master's degree in Electrical-Telecommunication Engineering from Telkom University, Bandung, Indonesia, in March 2012. Since 2010, he joined as a Lecturer in the Diploma of Telecommunication Technology, School of Applied Science, Telkom University. He is also currently a member of the Biomedical Instrumentation Research Group at Telkom University. His research interests are wireless sensor networks, embedded systems, logic design on FPGA, and biomedical engineering. In 2018-present, he became a doctoral student in electrical engineering at the Bandung Institute of Technology. The focus of his doctoral research is signal processing and analysis of EEG waves. Email: sugondo@telkomuniversity.ac.id, Orchid: https://orcid.org/my-orcid?orcid=0000-0002-2086-2156.